ISSN 1674-1056
http://cpb.iphy.ac.cn
http://iopscience.iop.org/cpb
中国物理 B
Chinese Physics
中国物理 Chinese Physics B

Mode-locked fiber laser with $MoSe_2$ saturable absorber based on evanescent field

Ren-Li Zhang(张仁栗), Jun Wang(王俊), Xiao-Yan Zhang(张晓艳), Jin-Tian Lin(林锦添), Xia Li(李夏), Pei-Wen Kuan(关珮雯), Yan Zhou(周延), Mei-Song Liao(廖梅松), Wei-Qing Gao(高伟清)

Citation: Chin. Phys. B . 2019, 28(1): 014207. **doi:** 10.1088/1674-1056/28/1/014207
Journal homepage: http://cpb.iphy.ac.cn; http://iopscience.iop.org/cpb

What follows is a list of articles you may be interested in

Carboxyl graphene oxide solution saturable absorber for femtosecond mode-locked erbium-doped fiber laser

Rui-dong Lv(吕瑞东), Lu Li(李璐), Yong-gang Wang(王勇刚), Zhen-dong Chen(陈振东), Si-cong Liu(刘思聪), Xi Wang(王茜), Jiang Wang(王江), Yong-fang Li(李永放)

Chin. Phys. B . 2018, 27(11): 114214. **doi:** 10.1088/1674-1056/27/11/114214

Femtosecond Tm-Ho co-doped fiber laser using a bulk-structured Bi_2Se_3 topological insulator

Jinho Lee(李珍昊), Ju Han Lee(李周翰)

Chin. Phys. B . 2018, 27(9): 094219. **doi:** 10.1088/1674-1056/27/9/094219

Two-dimensional materials-decorated microfiber devices for pulse generation and shaping in fiber lasers

Zhi-Chao Luo(罗智超), Meng Liu(刘萌), Ai-Ping Luo(罗爱平), Wen-Cheng Xu(徐文成)

Chin. Phys. B . 2018, 27(9): 094215. **doi:** 10.1088/1674-1056/27/9/094215

Reduced graphene oxide as saturable absorbers for erbium-doped passively mode-locked fiber laser

Zhen-Dong Chen(陈振东), Yong-Gang Wang(王勇刚), Lu Li(李璐), Rui-Dong Lv(吕瑞东), Liang-Lei Wei(韦良雷), Si-Cong Liu(刘思聪), Jiang Wang(王江), Xi Wang(王茜)

Chin. Phys. B . 2018, 27(8): 084206. **doi:** 10.1088/1674-1056/27/8/084206

Generation and evolution of multiple operation states in passively mode-locked thulium-doped fiber laser by using a graphene-covered-microfiber

Xiao-Fa Wang(王小发), Jun-Hong Zhang(张俊红), Xiao-Ling Peng(彭晓玲), Xue-Feng Mao(毛雪峰)

Chin. Phys. B . 2018, 27(8): 084215. **doi:** 10.1088/1674-1056/27/8/084215

Mode-locked fiber laser with $MoSe_2$ saturable absorber based on evanescent field*

Ren-Li Zhang(张仁栗)[1,2], Jun Wang(王俊)[1], Xiao-Yan Zhang(张晓艳)[1], Jin-Tian Lin(林锦添)[3], Xia Li(李夏)[1], Pei-Wen Kuan(关珮雯)[1], Yan Zhou(周延)[4], Mei-Song Liao(廖梅松)[1,†], and Wei-Qing Gao(高伟清)[5]

[1] *Key Laboratory of Materials for High Power Laser, Shanghai Institute of Optics and Fine Mechanics, Chinese Academy of Sciences, Shanghai* 201800, *China*

[2] *University of Chinese Academy of Sciences, Beijing* 100039, *China*

[3] *State Key Laboratory of High Field Laser Physics, Shanghai Institute of Optics and Fine Mechanics, Chinese Academy of Sciences, Shanghai* 201800, *China*

[4] *College of Science, Shanghai Institute of Technology, Shanghai* 201418, *China*

[5] *School of Electronic Science & Applied Physics, Hefei University of Technology, Hefei* 230009, *China*

(Received 28 August 2018; revised manuscript received 30 September 2018; published online 12 December 2018)

An all-fiber mode-locked fiber laser was achieved with a saturable absorber based on a tapered fiber deposited with layered molybdenum selenide ($MoSe_2$). The laser was operated at a central wavelength of 1558.35 nm with an output spectral width of 2.9 nm, and a pulse repetition rate of 16.33 MHz. To the best of our knowledge, this is the first report on mode-locked fiber lasers using $MoSe_2$ saturable absorbers based on tapered fibers.

Keywords: fiber lasers, mode locking, molybdenum diselenide

PACS: 42.55.Wd, 42.60.Fc, 78.67.–n **DOI:** 10.1088/1674-1056/28/1/014207

1. Introduction

Ultrafast fiber lasers have important applications in optical communication, material processing, sensing, and medical imaging.[1–5] The passive mode-locking technique is a major method for generating ultrashort optical pulses. It is more promising than active mode-locking techniques because of its compactness and simplicity.[6] There are several ways to achieve passively mode-locked fiber lasers, such as nonlinear polarization evolution (NPE),[7,8] nonlinear optical loop mirror (NOLM),[9,10] and semiconductor saturable absorber mirror (SESAM).[11–13] Compared to the first two methods, SESAM offers better stability and self-starting ability.[14] However, the narrow operating bandwidth, manufacturing complexity, and high cost of SESAM limit its applications as a mode-locking technique, thereby promoting research into new saturable absorbers (SA) such as carbon nanotubes and graphene.[14–17]

In 2009, graphene was used for the first time as an SA in ultrafast optics.[16] Thereafter, different kinds of two-dimensional (2D) materials have been developed and applied in passively mode-locked fiber lasers.[18–26] SAs based on 2D materials offer unique advantages such as simple manufacturing, wide response bandwidth, and short relaxation time.[27–30] In recent years, new kinds of 2D materials called transition metal dichalcogenides (TMDs) are attracting significant attention due to their interesting properties (e.g., layer-dependent bandgap).[31] TMDs can be expressed using the typical chemical formula MX_2, where M represents a transition metal (e.g., Mo, W) and X represents a chalcogen (e.g., S, Se). Among TMDs, molybdenum disulfide (MoS_2) and tungsten disulfide (WS_2) are most widely studied in ultrashort pulse fiber lasers. Mode-locked fiber lasers with TMD-based SAs were first reported by Zhang *et al.* in 2014, and was realized with a MoS_2-deposited fiber ferrule.[32] Since then, mode-locked fiber lasers with MoS_2/WS_2-based SAs have been extensively investigated at wavelengths of 1 μm, 1.5 μm, and 2 μm.[32–39]

Recently, molybdenum diselenide ($MoSe_2$), another member of the TMDs family, has shown its potential for application in mode-locking technology. The layered $MoSe_2$ has a broadband absorption that ranges from the visible light wavelength to the near-infrared wavelength regions. This gives $MoSe_2$ certain advantages over carbon nanotubes and would potentially makes $MoSe_2$ more suitable than MoS_2 as SA in passively mode-locked lasers.[14,19] However, there is limited research on $MoSe_2$ compared to MoS_2/WS_2. TMDs have lower thermal conductivities compared to graphene.[18] Therefore, optical damage becomes an important issue when considering the integration of TMDs with fiber lasers. A method that employs side-polished fibers (SPF) or tapered fibers offers a way to solve this problem. It utilizes the interaction between the evanescent field of the fiber and the material wrapped outside that prevents direct contact between the op-

*Project supported by the National Key Research and Development Program of China (Grant No. 2018YFB0504500), the National Natural Science Foundation of China (Grant Nos. 61475171, 61705244, 61307056, and 61875052), and the Natural Science Foundation of Shanghai, China (Grant Nos. 17ZR1433900 and 17ZR1434200).

†Corresponding author. E-mail: liaomeisong@siom.ac.cn

© 2019 Chinese Physical Society and IOP Publishing Ltd

tical field and the saturable absorbing material and effectively raises the damage threshold of the SAs. In addition, the methods based on SPF and tapered fiber are easy for packaging and therefore more suitable for the manufacturing of commercial mode-locking devices. Moreover, with careful design, SAs based on tapered fiber could have abnormal dispersion at the operating wavelength of the laser that would help to manage the net dispersion of the laser cavity.[40,41] There are several reports on mode-locked fiber lasers with $MoSe_2$ film or SPF.[19,42–44] However, there is no report on tapered-fiber-based $MoSe_2$ SAs.

In this paper, we demonstrate an all-fiber mode-locked fiber laser with a $MoSe_2$ SA based on tapered fiber. To the best of our knowledge, this is the first report on mode-locked fiber lasers using tapered fiber-based $MoSe_2$ SAs.

2. Fabrication of $MoSe_2$ SA

2.1. Preparation of the layered $MoSe_2$

Liquid phase exfoliation (LPE) is widely used in the fabrication of 2D materials because of its simplicity and effectiveness.[19,43] In our experiment, LPE was used to prepare few-layer $MoSe_2$ nanosheets. Initially, 200 mg of the bulk $MoSe_2$ was mixed with 40-ml N-methyl pyrrolidone (NMP) and the mixture was treated by one-hour ultrasonication to break the bulk $MoSe_2$ into layered flakes. The suspension obtained was then centrifuged for 90 min at a rotation speed of 3000 rpm. After the centrifugation, the upper clear liquid from the suspension was collected as the few-layered $MoSe_2$ dispersion.

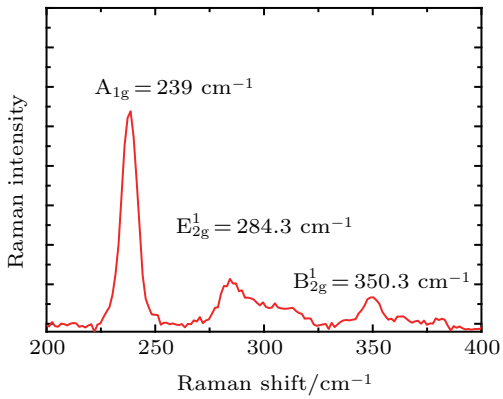


Fig. 1. Raman spectra of the $MoSe_2$ nanosheet.

To verify the effectiveness of the liquid phase exfoliation of $MoSe_2$, the Raman spectra of the dispersion were tested. The $MoSe_2$ dispersion was dropped on a glass substrate and dried and the Raman spectra were measured using an excitation wavelength of 488 nm. The result obtained is shown in Fig. 1. As can be seen in the Raman spectra, the A_{1g}, E^1_{2g}, and B^1_{2g} Raman peaks are located at 239 cm^{-1}, 284.3 cm^{-1}, and 350.3 cm^{-1}, respectively, confirming the existence of layered $MoSe_2$ with 1–5 layers.[45] The absorption spectra were recorded in a range of 500–1100 nm using a Lambda 950 UV–VIS–NIR spectrophotometer. As shown in Fig. 2, the two peaks at 695 nm and 800 nm further confirm the existence of layered $MoSe_2$.[43]

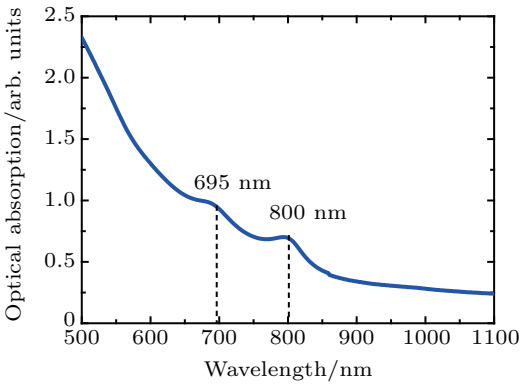


Fig. 2. Optical absorption of $MoSe_2$ nanosheet.

2.2. Simulation and fabrication of tapered fiber

The ratio of evanescent field power to total propagation power is determined by the waist diameter of the tapered fiber. The mode field distribution at the waist of the tapered fiber was simulated using finite element analysis. The wavelength and refractive index of the fiber cladding were set to be 1.55 μm and 1.45, respectively. Air, with a refractive index of 1, was taken as the medium surrounding the waist of the tapered fiber. The simulated result is shown in Fig. 3. It can be seen from the results that the ratio of the evanescent field power to the total power increases as the waist diameter of the tapered fiber decreases. To guarantee the effective interaction between the evanescent field and the material surrounding the fiber waist, the waist diameter needs to be small. Under the given experimental conditions, it is difficult to fabricate a tapered fiber with a relatively small loss and a waist diameter less than 3 μm. Therefore, the tapered fiber waist was taken to be 3 μm. The area of power of the evanescent field was about 1.2%, according to the simulation results.

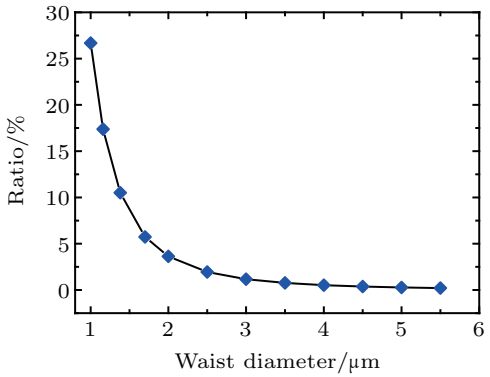


Fig. 3. Simulation result of relationship between the ratio of evanescent field power to total propagation power and tapered fiber waist diameter.

The tapered fiber used in our experiment was prepared by stretching a segment of a standard single mode fiber (SMF-28) using an oxyhydrogen flame. The waist diameter of the tapered fiber was measured as ~ 3 μm and the insertion loss as 0.4 dB at 1550 nm. The insertion loss was likely caused by the surface contamination of the fiber and nonuniform heating during tapering.

2.3. Optical deposition of layered $MoSe_2$

The optical deposition method was used to deposit the layered $MoSe_2$ onto the tapered fiber waist. A small volume of the dispersion was dropped on the tapered fiber waist. The tapered fiber was connected to a continuous-wave (CW) fiber laser at a wavelength of 1560 nm and a power of 26 mW. When the light of the CW laser propagated in the tapered fiber, the leakage of light field appeared in the waist region of the tapered fiber which was immersed in the dispersion droplet. Owing to the optical tweezer effect and light induced swirl and convection, the $MoSe_2$ nanosheets were trapped and deposited onto the tapered fiber. During the deposition, the tapered fiber was taken out of the droplet to measure the insertion loss at regular intervals. When the insertion loss rose to 4.8 dB, the laser was turned off and the deposition was completed. Using a microscope, the uneven deposition of several-micron-sized $MoSe_2$ nanosheets can be seen on the fiber waist with a distribution length of about 100 μm. Schematic illustrations of the optical deposition method and the tapered fiber deposited with layered $MoSe_2$ are shown in Figs. 4(a) and Fig. 4(b), respectively.

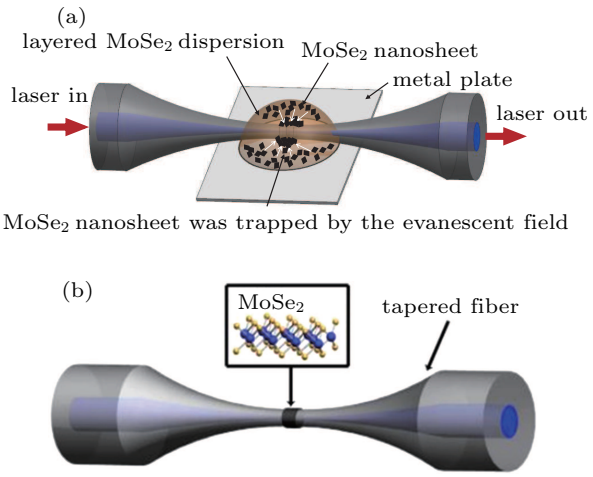


Fig. 4. Schematic illustrations of (a) the principle of optical deposition method and (b) a $MoSe_2$ SA based on a tapered fiber.

The nonlinear transmission of the $MoSe_2$ SA was measured using a balanced twin-detector system. The laser source used was a commercial passively mode-locked erbium-doped fiber laser with a pulse width of ~ 200 fs and a central wavelength of 1557 nm. The measured result is shown in Fig. 5.

Because of the limitation of the output power of our laser source, the $MoSe_2$ SA was not fully saturated in the measurement. The measured modulation depth of the $MoSe_2$ SA was around 0.8% and the unsaturated loss around 52%. These values are comparable to those obtained in reported works. As shown in Fig. 5, the highest input intensity is about 3900 MW/cm^2. With the decrease of the input power, the transmittance of the SA can repeat the data recorded during the rise of the input power. This means that the $MoSe_2$ SA has a damage threshold higher than 3900 MW/cm^2.

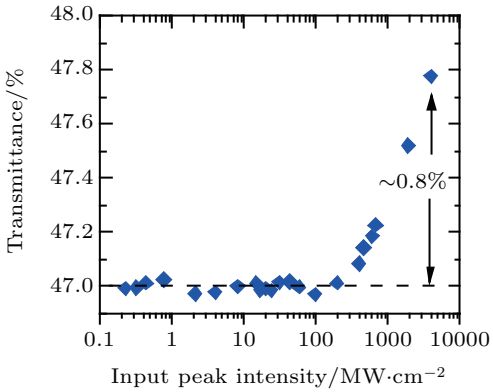


Fig. 5. Nonlinear transmission of $MoSe_2$ SA based on tapered fiber.

3. Mode-locked fiber laser with $MoSe_2$ SA

3.1. Experimental setup

An erbium-doped mode-locked fiber laser with $MoSe_2$ SA was set up as shown in Fig. 6. A laser diode operating at a wavelength of 980 nm was connected to a 980/1550 wavelength division multiplexer (WDM). A polarization-independent isolator (ISO) was used to ensure unidirectional operation. A polarization controller (PC) was spliced in the cavity to control cavity polarization. The output pulse was coupled out of the cavity using the 20% fiber of the 20/80 output coupler (OC). The whole cavity consisted of 0.65-m erbium-doped fiber (Nufern SM-ESF-7/125) and about 12-m single-mode fiber (SMF-28). The group velocity dispersions (GVDs) of the erbium-doped fiber and SMF-28 were −0.02 ps^2/m and −0.022 ps^2/m, respectively at 1550 nm. Using finite element analysis, the GVD of our tapered fiber waist

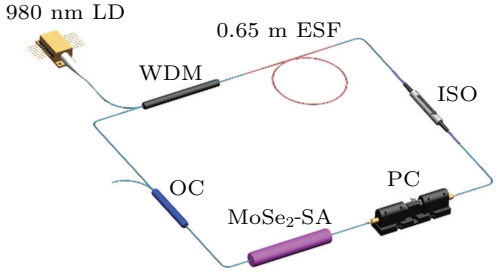


Fig. 6. Experimental setup of mode-locked fiber laser with $MoSe_2$ SA.

was calculated to be -0.166 ps^2/m, a value that is about 8 times higher than the one before the tapering. Despite the high GVD of the tapered waist, its short length makes the dispersion of the tapered fiber very small. Therefore, its effect on the laser operation is negligible. The net cavity dispersion was estimated as -0.278 ps^2.

3.2. Result and discussion

When the pump power reached 30.7 mW, the mode-locking pulse could be easily obtained with proper adjustment of the PC with an output power of 0.2 mW. The laser could operate in the fundamental mode-locking state until the pump power reached 79.8 mW. Further increment in the pump power caused the mode-locked laser to operate in an unstable multi-pulse mode-locking regime. The output spectrum measured using an optical spectrum analyzer (OSA Yokogawa AQ6370C) is shown in Fig. 7.

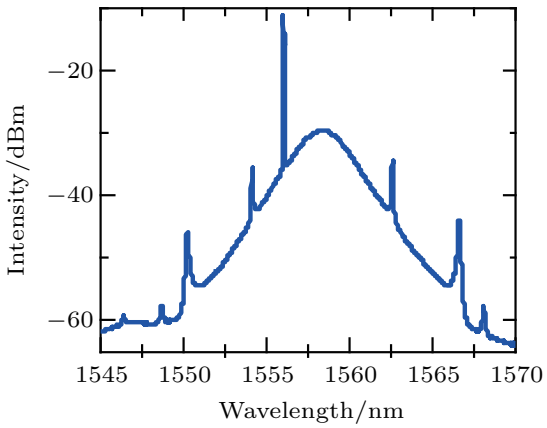


Fig. 7. Output spectrum.

When the laser is operated under the pump power of 37 mW, the output spectrum is centered at 1558.35 nm with a 3-dB bandwidth of 2.9 nm. The spectrum has typical Kelly sidebands, indicating that the output pulse is a traditional soliton. As can be seen in the output spectrum, a CW component exists at the wavelength of 1556 nm. A similar phenomenon was also observed in reported works with Bi_2Te_3,[24] SWNT,[46] and MoS_2.[47] Figure 8 shows the output pulse train measured with a 1 GHz digital oscilloscope (Tektronic MDO 3102). The interval of the pulses train is 61.2 ns, corresponding to a repetition rate of 16.33 MHz and a cavity length of 12.67 m, thereby proving the single-pulse operation of the mode-locked laser. As shown in the figure, the peak intensity of the output pulses is not constant. These fluctuations were likely caused by a fraction of output laser fed back to the laser cavity.[48] The corresponding radio frequency (RF) spectrum was measured with a resolution bandwidth (RBW) of 50 Hz, as shown in Fig. 9. The pulse repetition rate was 16.33 MHz while the signal-to-noise ratio was 52 dB.

Prior to our investigation, there have been several reports on erbium-doped mode-locked fiber lasers realized using TMD-based saturable absorbers. Details of these reports are listed below. Comparable results were obtained in our tapered-fiber $MoSe_2$ SA experiment as outlined at the bottom of the list.

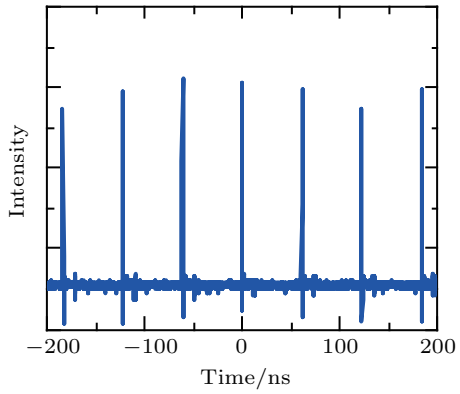


Fig. 8. Output pulse train.

Table 1. Output performance of reported erbium-doped mode-locked fiber lasers incorporating with TMD-based saturable absorbers. TF is tapered fiber.

Ref.	SA form	Spectral width/nm	Pulse duration/ps	Modulation depth/%
[49]	MoS_2-TF	2.47	–	2.82
[50]	WS_2-TF	6.75	0.609	7.8
[21]	WSe_2 film	2.1	1.25	0.5
[21]	WSe_2-SPF	2	1.31	0.3
[22]	$MoTe_2$ film	2	–	0.9
[22]	$MoTe_2$-SPF	2.4	1.2	1.8
[22]	WTe_2 film	2	–	1.5
[22]	WTe_2-SPF	2	–	2.8
[51]	ReS_2 film	2.47	1.2	0.14
[52]	SnS_2 film	6.09	0.623	4.6
[19]	$MoSe_2$ Film	1.75	1.45	0.63
[43]	$MoSe_2$ film	7.8	0.58	7.3
[42]	$MoSe_2$-SPF	5.4	0.798	5.4
[21]	$MoSe_2$-SPF	2.3	1.09	1.4
[21]	$MoSe_2$ film	2.2	1.18	0.4
This work	$MoSe_2$-TF	2.9	~ 1	0.8

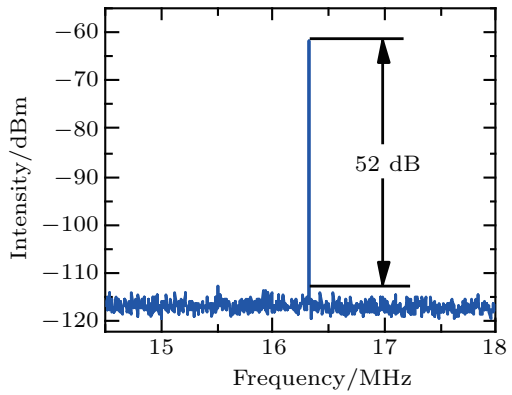


Fig. 9. RF spectrum.

The duration of the output pulse could not be measured directly because the output power was too low for the autocorrelator used in the experiment. However, it can be estimated using existing information. Based on the 3-dB bandwidth of the output spectrum shown in Fig. 7, the transform limited pulse duration can be calculated as 879 fs. Moreover, the output pulse obtained in the experiment is the traditional soliton, meaning that the pulse is slightly chirped. Therefore, considering the transform limited pulse duration, the slight chirp of the pulse, and the pulse width of the results with similar spectral bandwidth listed in Table 1, the pulse duration can be estimated as around 1 ps.

4. Conclusion

An all-fiber erbium-doped mode-locked fiber laser with a $MoSe_2$ SA was demonstrated in this paper. The SA was based on evanescent field interaction, realized with a tapered fiber deposited with layered $MoSe_2$. The modulation depth and unsaturated loss of the $MoSe_2$ SA were about 0.8% and 52%. The output pulse obtained in our experiment was a traditional soliton with a 3-dB bandwidth of 2.9 nm and a repetition rate of 16.33 MHz. Our work indicates that based on evanescent field interaction, tapered fiber coated with layered $MoSe_2$ can be used as an effective saturable absorber for mode locking.

References

[1] Keller U 2003 *Nature* **424** 831
[2] Chong A, Wright L G and Wise F W 2015 *Rep. Prog. Phys.* **78** 113901
[3] Oktem B, Ülgüdür C and Ö F 2010 *Nat. Photon.* **4** 307
[4] Liu X, Cui Y, Han D, Yao X and Sun Z 2015 *Sci. Rep.* **5** 9101
[5] Liu X, Han D, Sun Z, Zeng C, Lu H, Mao D, Cui Y and Wang F 2013 *Sci. Rep.* **3** 2718
[6] Ahmed M H, Latiff A A, Arof H and Harun S W 2016 *Appl. Opt.* **55** 4247
[7] Ilday F Ö, Buckley J, Kuznetsova L and Wise F W 2003 *Opt. Express* **11** 3550
[8] Chong A 2006 *Opt. Express* **14** 10095
[9] Song Wu, Jefferson Strait and Fork R L 1993 *Opt. Lett.* **18** 1444
[10] Ö F and Wise F W 2002 *Opt. Lett.* **27** 1531
[11] Gomes L A, Orsila L, Jouhti T and Okhotnikov O G 2004 *IEEE J. Sel. Top. Quantum Electron.* **10** 129
[12] Keller U 1996 *IEEE J. Sel. Top. Quantum Electron.* **2** 435
[13] Xiao X S 2017 *Chin. Phys. B* **26** 114204
[14] Martinez A and Sun Z 2013 *Nat. Photon.* **7** 842
[15] Liu X, Yao X and Cui Y 2018 *Phys. Rev. Lett.* **121** 023905
[16] Bao Q, Zhang H, Wang Y, Ni Z, Yan Y, Shen Z X, Loh K P and Tang D Y 2009 *Adv. Funct. Mater.* **19** 3077
[17] Yamashita S and Inoue Y 2004 *Opt. Lett.* **29** 1581
[18] Du J, Wang Q, Jiang G, Xu C, Zhao C, Xiang Y, Chen Y, Wen S and Zhang H 2015 *Sci. Rep.* **4** 6346
[19] Luo Z, Li Y, Zhong M, Huang Y, Wan X, Peng J and Weng J 2015 *Photon. Res.* **3** A79
[20] Mao D, Wang Y, Ma C, Han L, Jiang B, Gan X, Hua S, Zhang W, Mei T and Zhao J 2015 *Sci. Rep.* **5** 7965
[21] Mao D, She X, Du B, Yang D, Zhang W, Song K, Cui X, Jiang B, Peng T and Zhao J 2016 *Sci. Rep.* **6** 23583
[22] Mao D, Du B, Yang D, Zhang S, Wang Y, Zhang W, She X, Cheng H, Zeng H and Zhao J 2016 *Small* **12** 1489
[23] Zhao C J, Zou Y H, Chen Y, Wang Z T, Lu S B, Zhang H, Wen S C and Tang D Y 2012 *Opt. Express* **20** 27888
[24] Luo Z C, Liu M, Liu H, Zheng X W, Luo A P, Zhao C J, Zhang H, Wen S C and Xu W C 2013 *Opt. Lett.* **38** 5212
[25] Sotor J, Sobon G, Kowalczyk M, Macherzynski W, Paletko P and Abramski K M 2015 *Opt. Lett.* **40** 3885
[26] Park K, Lee J, Lee Y T, Choi W, Lee J H and Song Y 2015 *Ann. Phys.-Berlin* **527** 770
[27] Xin W, Liu Z B, Sheng Q W, Feng M, Huang L G, Wang P, Jiang W S, Xing F, Liu Y G and Tian J G 2014 *Opt. Express* **22** 10239
[28] Xing G, Guo H, Zhang X, Sum T C and Huan C H A 2010 *Opt. Express* **18** 4564
[29] Shi H, Yan R, Bertolazzi S, Brivio J, Gao B, Kis A, Jena D, Xing H G and Huang L 2013 *ACS Nano* **7** 1072
[30] Tran V, Soklaski R, Liang Y and Yang L 2014 *Phys. Rev. B* **89** 235319
[31] Wang Q H, Kalantar-Zadeh K, Kis A, Coleman J N and Strano M S 2012 *Nat. Nanotechnol.* **7** 699
[32] Zhang H, Lu S B, Zheng J, Du J, Wen S C, Tang D Y and Loh K P 2014 *Opt. Express* **22** 7249
[33] Khazaeizhad R, Kassani S H, Jeong H, Yeom D I and Oh K 2014 *Opt. Express* **22** 23732
[34] Tian Z, Wu K, Kong L, Yang N, Wang Y, Chen R, Hu W, Xu J and Tang Y 2015 *Laser Phys. Lett.* **12** 065104
[35] Jung M, Lee J, Park J, Koo J, Jhon Y M and Lee J H 2015 *Opt. Express* **23** 19996
[36] Mao D, Zhang S, Wang Y, Gan X, Zhang W, Mei T, Wang Y, Wang Y, Zeng H and Zhao J 2015 *Opt. Express* **23** 27509
[37] Guo B, Yao Y, Yan P, Xu K, Liu J, Wang S and Li Y 2016 *IEEE Photon. Technol. Lett.* **28** 323
[38] Liu M, Luo A, Xu W and Luo Z 2018 *Chin. Opt. Lett.* **16** 020008
[39] Kadir N A A, Ismail E I, Latiff A A, Ahmad H, Arof H and Harun S W 2017 *Chin. Phys. Lett.* **34** 014202
[40] Rusu M, Herda R, Kivistö S and Okhotnikov O G 2006 *Opt. Lett.* **31** 2257
[41] Wang L, Xu P, Li Y, Han J, Guo X, Cui Y, Liu X and Tong L 2018 *Sci. Rep.* **8** 4732
[42] Koo J, Park J, Lee J, Jhon Y M and Lee J H 2016 *Opt. Express* **24** 10575
[43] Ahmad H, Aidit S N, Hassan N A, Ismail M F and Tiu Z C 2016 *Opt. Eng.* **55** 076115
[44] Tiu Z C, Ahmad H, Zarei A and Harun S W 2016 *Chin. Opt. Lett.* **14** 041901
[45] Chen B, Zhang X, Wu K, Wang H, Wang J and Chen J 2015 *Opt. Express* **23** 26723
[46] Gui L, Yang X, Zhao G, Yang X, Xiao X, Zhu J and Yang C 2011 *Appl. Opt.* **50** 110
[47] Xia H D, Li H P, Lan C Y, Li C, Deng G L, Li J F and Liu Y 2015 *Chin. Phys. B* **24** 084206
[48] Wang G 2017 *Opt. Laser Technol.* **96** 307
[49] Liu M, Zheng X W, Qi Y L, Liu H, Luo A P, Luo Z C, Xu W C, Zhao C J and Zhang H 2014 *Opt. Express* **22** 22841
[50] Chen H, Li I L, Ruan S, Guo T and Yan P 2016 *Opt. Eng.* **55** 081318
[51] Mao D, Cui X, Gan X, Li M, Zhang W, Lu H and Zhao J 2018 *IEEE J. Sel. Top. Quantum Electron.* **24** 1100406
[52] Niu K, Sun R, Chen Q, Man B and Zhang H 2018 *Photon. Res.* **6** 72